ISSN 2616-5880 Vol. 6, Issue 2: 25-32, DOI: 10.25236/AJMC.2025.060203

Phase Relationship in the Ho–Sn–Ti ternary system close to the Ho–Ti side at 1000 °C

Gong Guanhua, Cui Xuehong*, Liang Jianlie

School of Materials and Environment, Guangxi Key Laboratory of Advanced
Key Laboratory of Eco-friendly Materials and Ecological Restoration, Guangxi Minzu University, Nanning 530105, China
**Corresponding author: cxh841113@163.com*

Abstract: *The phase relationship of the Ho–Sn–Ti ternary system close to the Ho–Ti side at 1000 °C was investigated by means of X-ray diffraction, scanning electron microscopy, and energy-dispersive X-ray spectroscopy. Two new ternary compounds were discovered, namely $HoSn_4Ti_6$ and ε($Ho_{11}Sn_{44}Ti_{45}$). The $HoSn_4Ti_6$ phase adopts a structure type analogous to $GdSn_4Ti_6$, with lattice constants of a = 0.58178(3) nm and c = 2.28814(6) nm. The structure phase ε is unknown. Meanwhile, the existences of 5 binary compounds (i.e. Ti_6Sn_5, Ti_5Sn_3, Ti_2Sn, Ti_3Sn, and Ho_5Sn_3) were confirmed. The maximum solid solubility of Ti in Ho_5Sn_3 was about 10.5 at.%.*

Keywords: *Phase diagram; Titanium alloys; Ho–Sn–Ti system*

1. Introduction

Titanium alloys are characterized by high strength and light weight, excellent corrosion resistance, high heat resistance and low density, and are widely used in aerospace[1], military[2] and biomedical applications[3]. In the process of further improving the properties of titanium alloys, people have applied methods such as multi-element alloying, and found that if a small amount of rare earth elements are doped, the microstructure and properties of titanium alloys can be significantly improved. It is reported that the addition of a small amount of Ho can refine the grain size, improve oxidation resistance and hydrogen absorption capacity[4]. The researchers found that adding a small amount of Sn can improve the yield strength, flexural strength, flexural modulus and ductility of titanium alloys[5]. The addition of Sn in the Ti-Nb alloys was observed to lead to the precipitate of Ti_3Sn, which provided significant strengthening effect for the alloys. The grain refining and precipitation strengthening are the two approaches to strength the alloys[6]. According to the above, the interaction between Ho and Sn on Ti alloys will have the effect of grain refinement and precipitation strengthening. To understand the synergistic effect of Ho and Sn, it is important to know the phase diagram of the Ho-Sn-Ti system.

There is no binary compound in the Ho–Ti system. In the Ho–Sn system, M.V. Bulanova et al. established the Ho-Sn phase diagram including six intermetallic compounds, i.e., Ho_5Sn_4, $Ho_{11}Sn_{10}$, Ho_4Sn_5, $HoSn_2$, Ho_2Sn_5, $HoSn_3$[7]. Ho_5Sn_3 melts at 1915 degrees Celsius and eutectic reaction at 1265 degrees Celsius[8], $HoSn_2$, Ho_2Sn_5, and $HoSn_3$ form peritectically at 1130 ℃, 520 ℃, and 420 ℃ respectively[9]. In the Ho–Cu–Sn[10] and Ho–Sn–Fe[11] ternary systems, the presence of Ho_5Sn_3, $Ho_{11}Sn_{10}$, $HoSn_2$, and Ho_2Sn_5 was reported.

The Sn-Ti system was first thermodynamically evaluated by Murray[12]. The binary system contained four intermetallic compounds, Ti_6Sn_5, Ti_5Sn_3, Ti_2Sn, and Ti_3Sn. When Kuper[13] reexamined the binary Sn-Ti system, they found a new binary compound Ti_2Sn_3, which was later confirmed by O'Brien[14].

Until now, the phase diagram of the Ho-Sn-Ti system is still unknown. The purpose of this study is to investigate the phase diagram of the Ho-Sn-Ti system.

2. Experimental details

All 14 alloy ingots were made by arc melting using non-consumable tungsten electrodes on water-cooled copper crucibles in a pure argon atmosphere. Zirconium was used as an oxygen capture agent during the melting process. The total weight of each specimen was 1.5 grams. The starting materials used were Ho (99.9 wt.%), Sn (99.9 wt.%) and Ti (99.9 wt.%). Each specimen was melted three times to

ISSN 2616-5880 Vol. 6, Issue 2: 25-32, DOI: 10.25236/AJMC.2025.060203

ensure homogeneity. The weight loss of the melted alloys was less than 1.5%. The ingots were sealed in evacuated quartz tubes and annealed at 1000 °C for 60 days. After annealing, the samples were quenched in water. X-ray diffraction (XRD) was performed on a diffractometer (Bruker Advance-D8) using Cu Kα with a tube voltage of 40 kV and a current of 40 mA. Microstructural analyses of the samples were performed using a scanning electron microscope (SEM, ZEISS EVO 18) equipped with an energy dispersive spectrometer (EDS, Bruker Nano XFlash Detector 5010). to analyze the microstructure of the samples. Lattice constants were calculated by the least squares method. Rietveld analysis was performed using Fullprof [15].

3. Results and discussion

3.1. New ternary compounds

Table 1 summarizes the composition of the alloys selected for this experiment, the calculated lattice parameters and the identified phases. After quenching at high temperatures, (Sn) can be observed to appear on the surface of the samples. The (Sn) precipitation on the surface of the ingot is due to reverse segregation of the liquid, a phenomenon usually found in alloys containing low-melting-point elements (e.g., tin, indium). To emphasize the presence of phases in this system, Table 1 lists some results for non-equilibrium and cast alloys.

Table 1: Summary of experimental results of XRD for the selected alloys.

No.	Nominal composition (at.%)			Phase	Space group	Composition (at.%)			Lattice parameters (nm)		
	Ho	Sn	Ti			Ho	Sn	Ti	*a*	*b*	*c*
1	28	5	67	Ho_5Sn_3	*P63/mcm*	60.2	35.6	4.2	0.8786(1)		0.6440(8)
				(βTi)	*P63/mcm*	0.2	0.1	99.6	0.2949(7)		0.4702(5)
				(Ho)	*P63/mmc*	93.7	5.9	0.4	0.3563(2)		0.5606(4)
2	17	18	65	Ho_5Sn_3	*P63/mmc*	61.1	34.6	4.3	0.8793(4)		0.6437(4)
				Ti_3Sn	*P63/mcm*	1.5	17.3	81.2	0.5859(5)		0.4760(8)
				(βTi)	*P63/mcm*	0.2	6.8	93.0	0.2954(5)		0.4695(9)
3	2	30	68	Ti_2Sn	*P63/mmc*	0.1	30.2	69.7	0.4650(3)		0.5706(4)
				Ti_3Sn	*P63/mcm*	0.1	21.5	78.4	0.5855(4)		0.4764(5)
				$HoSn_4Ti_6$	*R-3m*	7.8	32.8	59.4	0.5818(3)		2.2886(5)
4	5	37	58	Ti_5Sn_3	*P63/mcm*	1.8	35.2	63.0	0.8053(6)		0.5455(6)
				Ti_2Sn	*P63/mmc*	0.2	33.5	66.3	0.4653(6)		0.5687(5)
				$HoSn_4Ti_6$	*R-3m*	6.7	32.4	60.9	0.5796(4)		2.2843(7)
5[c]	9	36	55	$HoSn_4Ti_6$	*R-3m*	7.8	33.6	58.6	0.5817(5)		2.2884(6)
6	3	39	58	Ti_6Sn_5	*P63/mmc*	0.1	42.5	57.4	0.9213(3)		0.5688(1)
				Ti_5Sn_3	*P63/mmc*	0.1	35.3	64.7	0.8049(1)		0.5460(3)
				$HoSn_4Ti_6$	*R-3m*	6.1	33.5	60.4	0.5785(4)		2.2894(1)
7[ab]	25	32	43	$HoSn_4Ti_6$	*R-3m*	7.2	34.9	58.9	0.5826(7)		2.2880(5)
				Ti_3Sn	*P63/mmc*	0.2	21.4	79.4	0.5855(6)		0.4767(9)
				Ho_5Sn_3	*P63/mcm*	52.3	37.2	10.5	0.8758(6)		0.6375(2)
				(Sn)	*I41/amd*	…	…	…	0.5831(7)		0.3181(4)
8[ab]	33	39	28	$HoSn_4Ti_6$	*R-3m*	7.8	33.5	58.7	0.5896(4)		0.2879(1)
				Ho_5Sn_3	*P63/mcm*	59.4	33.9	6.7	0.8733(4)		0.6357(1)
				ε	*Unknown*	12.1	44.2	43.7	…		…
				Ti_6Sn_5	*P63/mmc*	0.4	42.8	53.2	0.9218(6)		0.5647(7)
				(Sn)	*I41/amd*	…	…	…	0.5827(1)		0.3174(3)
9	10	41	49	$HoSn_4Ti_6$	*R-3m*	7.4	32.8	60.8	0.5854(8)		2.2875(6)
				Ti_6Sn_5	*P63/mcm*	0.5	40.9	58.6	0.9203(7)		0.5679(9)
				ε	*unknown*	11.1	43.8	45.1	…		…
10[b]	16	40	44	Ho_5Sn_3	*P63/mcm*	60.8	34.5	4.7	0.8684(1)		0.6398(7)
				Ti_6Sn_5	*P63/mmc*	0.3	42.3	57.4	0.9198(4)		0.5702(1)
				$HoSn_4Ti_6$	*P63/mmc*	7.6	32.9	59.5	0.5805(4)		2.3275(2)
				ε	*unknown*	12.1	43.2	44.7	…		…
11[b]	21	50	49	Ti_6Sn_5	*P63/mmc*	0.3	42.5	57.2	0.9169(7)		0.5690(6)
				Ho_5Sn_3	*P63/mcm*	severe oxidation			0.8769(4)		0.6491(3)
				$HoSn_4Ti_6$	*R-3m*	8.2	31.4	60.4	0.5845(2)		2.2989(0)
				ε	*unknown*	11.2	44.1	44.7	…		…
12[d]	11	43	46	$HoSn_2$	*Cmcm*	31.4	68.3	0.3	0.4356(4)	1.6005(6)	0.4282(9)
				Ti_6Sn_5	*P63/mmc*	0.2	43.5	56.3	0.9137(3)		0.5686(2)
				ε	*unknown*	11.5	44.3	44.2	…		…

a. (Sn) precipitate on the surface of ingots due to the inverse segregation of liquid during the quench.
b. The equilibrium un-reached.
c. The alloys are annealed at 1000 °C for 7 days.
d. As-cast

Two new ternary compounds have been identified in this study, namely $HoSn_4Ti_6$ and ε. An unknown

ISSN 2616-5880 Vol. 6, Issue 2: 25-32, DOI: 10.25236/AJMC.2025.060203

set of diffraction peaks were observed in alloys 7-11 and the corresponding diffraction spectra will be presented in the next section. These diffraction peaks closely match those of $GdSn4Ti_6$[16]. Considering the adjacent positions of the elements Ho and Gd in the periodic table and the similarity between the Ho-Sn-Ti and Gd-Sn-Ti systems, it can be concluded that a new ternary compound, $HoSn_4Ti_6$, exists in the system.The SEM micrographs and XRD patterns of a single $HoSn_4Ti_6$ are shown in Fig. 1.

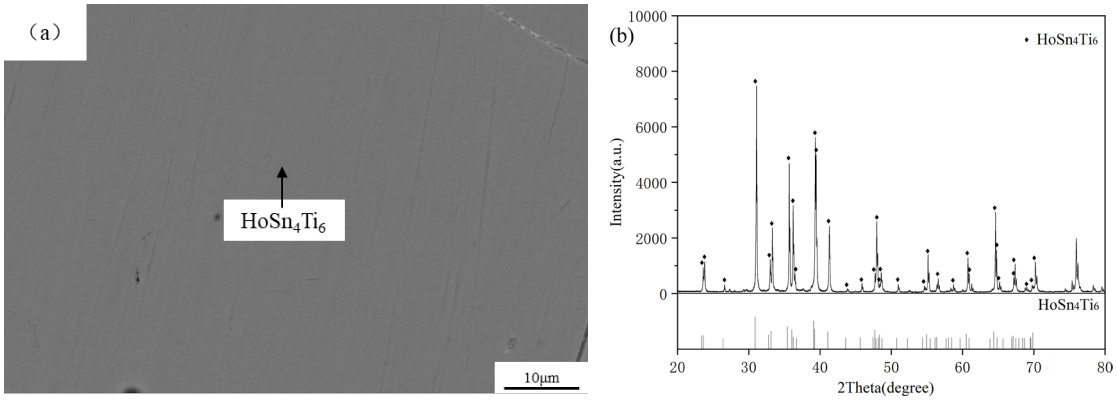

Fig. 1. The experimental results of alloy 7 ($Ho_{9.0}Sn_{36.0}Ti_{55.0}$) heated at 1000 ℃ for 60 days, (a) SEM micrograph, and (b) XRD pattern.

The indexing of the XRD pattern for the single phase was carried out using the Fullprof program, yielding lattice parameters of a = 0.57729(3) nm and c = 2.26839(6) nm. Taking the initial structure of $GdSn_4Ti_6$ (space group R-3m) as a reference, structural refinement was performed using the Fullprof software [15]. During the refinement process, a Pseudo-Voigt peak shape function was used for the structural refinement of $HoSn_4Ti_6$. Parameters such as scale factor, cell parameters, zero drift, background, etc. have been refined. The observed, calculated data and differences of the powder diffraction patterns of the new phase $HoSn_4Ti_6$ are shown in Fig.2. The results of the Rietveld structure refinement are presented in Table 2. The pattern R-factor (R_p) and the weighted pattern R-factor (R_{wp}) are R_p = 10.9 % and R_{wp} = 14.10 %, respectively.

Table 2: Rietveld structural refinement data of $HoSn_4Ti_6$.

Space group			R-3m (no. 166)			
Cell parameters			$a = b$ = 0.58178(3) nm, c = 2.28814(6) nm, α = β = 90°, γ = 120°			
Volume of unit cells (nm^3)			0.67071			
Calculated density (g/cm^3)			7.096			
Reliability factors (R-factor)			R_P = 13.30%, R_{WP} = 17.10%, R_{EXP} = 6.89%, Chi^2 = 6.09			
Atom parameters						
Atom	Positions	x	y	z	Occ.	B_{iso}
Ho	3a	0	0	0	1	1.08632
Sn	6c	0	0	0.33229	1	0.56045
Sn	6c	0	0	0.12791	1	1.11373
Ti	18h	0.49632	0.50368	0.10630	1	0.74346

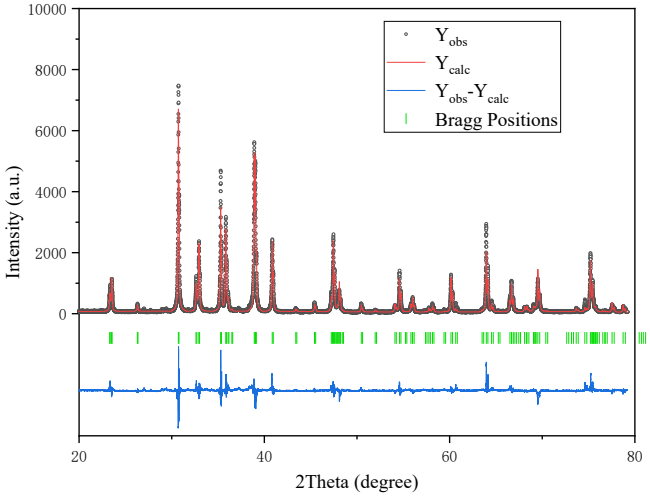

Fig. 2. Rietveld analysis of powder X-ray diffraction of ternary compound $HoSn_4Ti_6$.

ISSN 2616-5880 Vol. 6, Issue 2: 25-32, DOI: 10.25236/AJMC.2025.060203

The composition of the ε-phase in alloy 9 is 11.1 at.% Ho, 44.8 at.% Sn, and 44.1 at.% Ti, as shown in Table 1. Similar phase composition ratios were found in cast sample 12. In order to synthesize a single phase of this compound, alloy 11 ($Ho_{11}Sn_{43}Ti_{46}$) was prepared and then annealed at 1000°C for 7 days. No single phase ternary compound was obtained due to tin segregation. The ε phase occurs in annealed alloy 9 and cast alloy 12 as shown in Figure 3. The coexistence of the ε phase with the Ti_6Sn_5 phase was observed in both the annealed alloy 11 and the cast alloy 12, ruling out the possibility that the ε phase is a solid solution of Ho in the Ti_6Sn_5 phase. Alloy 11 consists of Ti_6Sn_5, ε, $HoSn_4Ti_6$ and Ho_5Sn_3. The light phase in alloy 11 is an oxidation product of Ho_5Sn_3. Although Alloy 11 is in equilibrium, the results confirm the presence of ε. Diffraction of this new ternary compound is difficult to determine due to the high degree of oxidation of the tin and tin-containing alloys. Figure 4 shows the X-ray diffraction patterns of alloys 9-11. As shown in Figure 4, as-cast alloy 12 contains peaks in the ε phase and fewer unknown peaks. By analyzing the X-ray diffractograms of alloys 9-11, the diffraction peaks at 33.958°, 34.327°, 37.339°, 39.464°, 48.048°, 48.776°, 55.572°, and 60.572° belong to the ε phase.

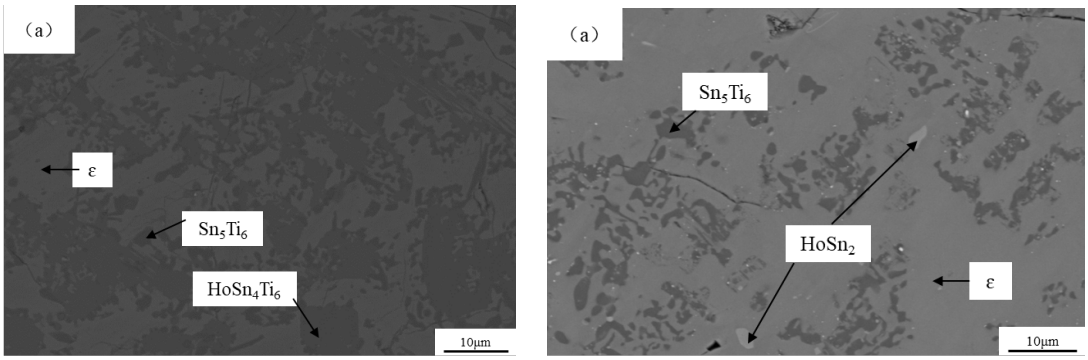

Fig. 3. BSE images of the selected samples, (a) alloy 9($Ho_{10.0}Sn_{41.0}Ti_{49.0}$) annealed at 1000°C for 7 days, and (b) as-cast alloy 12($Ho_{10.0}Sn_{60.0}Ti_{30.0}$).

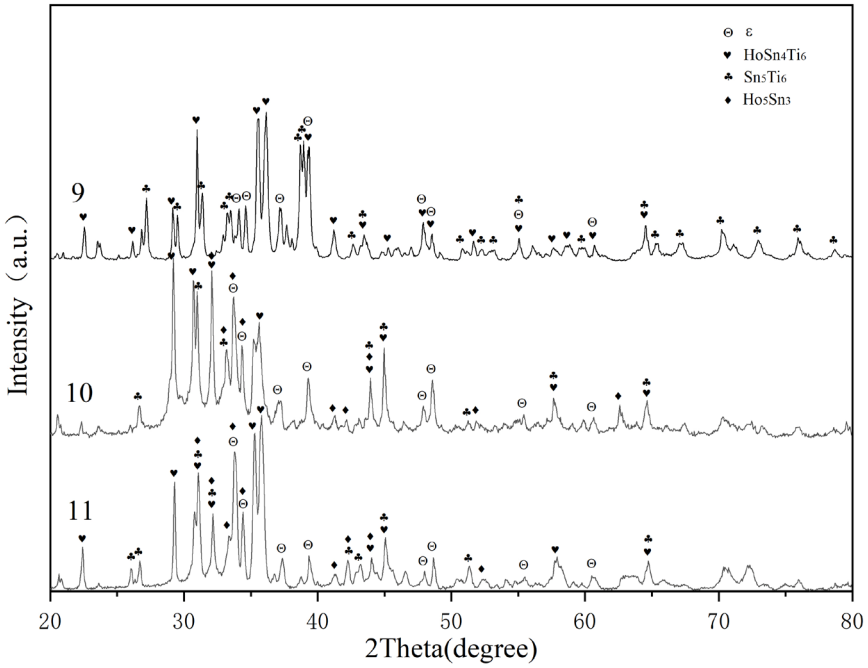

Fig. 4. The XRD pattern of alloy 9 ($Ho_{10.0}Sn_{41.0}Ti_{49.0}$), alloy 10 ($Ho_{16.0}Sn_{40.0}Ti_{44.0}$), alloy 11 ($Ho_{21.0}Sn_{50.0}Ti_{49.0}$).

3.2. Phase analysis

An XRD pattern of alloy 7 ($Ho_{25.0}Sn_{32.0}Ti_{43.0}$) is shown in Fig. 5. The XRD results indicate that the alloy is in the three-phase region of Ti_3Sn + $HoSn_4Ti_6$ + Ho_5Sn_3.

The XRD spectra of alloy 8 ($Ho_{33.0}Sn_{39.0}Ti_{28.0}$) are analyzed in detail in Fig. 6. The results show that

ISSN 2616-5880 Vol. 6, Issue 2: 25-32, DOI: 10.25236/AJMC.2025.060203

the alloy contains Ti_6Sn_5, $HoSn_4Ti_6$, Ho_5Sn_3. In addition, (Sn) and Ho_2O_3 were observed in alloy 8. It is difficult to avoid the presence of (Sn) and Ho_2O_3 in alloys containing tin and rare earth metals. The presence of (Sn) is due to the reverse segregation of the liquid during solidification. Alloys containing rare earth metals tend to oxidize when exposed to air during powder preparation, leading to the presence of Ho_2O_3.

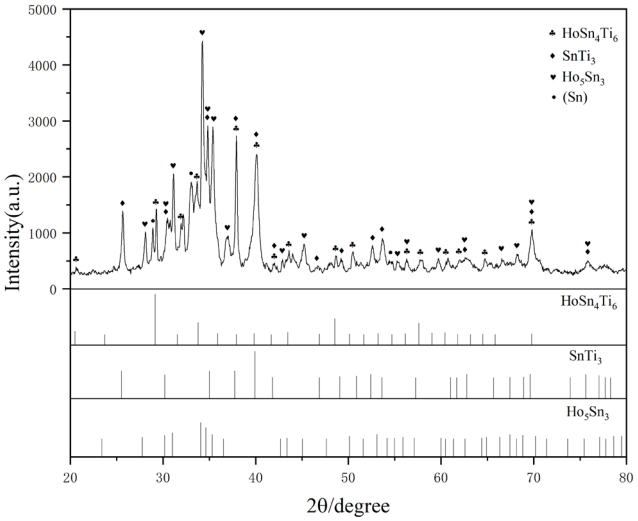

Fig. 5. The XRD pattern of alloy 7 ($Ho_{25.0}Sn_{32.0}Ti_{43.0}$).

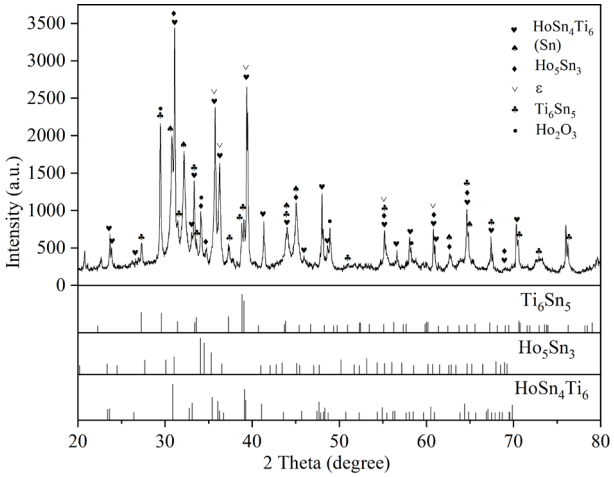

Fig. 6. The XRD pattern of alloy 8 ($Ho_{33.0}Sn_{39.0}Ti_{28.0}$).

The SEM morphology of alloy 4 ($Ho_{5.0}Sn_{37.0}Ti_{58.0}$) is shown in Fig. 7(a). According to the SEM/EDX analysis results, three phases, $HoSn_4Ti_6$, Ti_5Sn_3 and Ti_2Sn, can be observed. The gray phase is Ti_5Sn_3, the light gray phase is $HoSn_4Ti_6$, and the dark gray phase is Ti_2Sn. As shown in Fig. 7(b), the XRD spectra confirm these results. Fig. 8(a) shows the SEM morphology of alloy 6 ($Ho_{3.0}Sn_{39.0}Ti_{58.0}$) in which three phases, $HoSn_4Ti_6$, Ti_3Sn and Ti_2Sn are observed. The dark gray phase is Ti_3Sn, the gray phase is Ti_2Sn and the light colored phase is $HoSn_4Ti_6$.The presence of these phases is also confirmed by the XRD analysis results as shown in Fig. 8(b).

Fig. 9 are the SEM micrograph and XRD pattern of alloy 2 ($Ho_{17.0}Sn_{18.0}Ti_{65.0}$). As can be seen from Fig. 9(a), black-gray (βTi), dark-gray Ti_3Sn and gray Ho_5Sn_3 are observed.The XRD results shown in Fig. 9(b) are in agreement with the compositional analysis. Therefore, it can be concluded that alloy 9 is located in the three-phase region of (βTi) + Ti_3Sn + Ho_5Sn_3 .

ISSN 2616-5880 Vol. 6, Issue 2: 25-32, DOI: 10.25236/AJMC.2025.060203

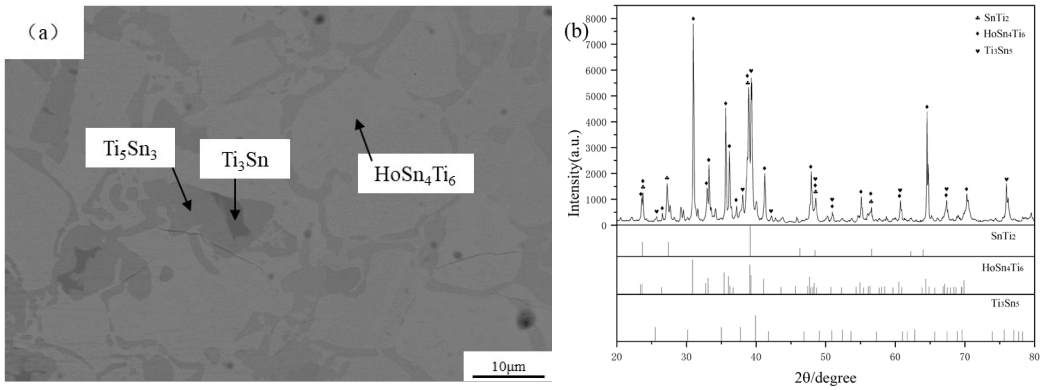

Fig. 7. The experimental results of alloy 4 ($Ho_{4.0}Sn_{36.0}Ti_{60.0}$) heated at 1000 ℃ for 60 days, (a) SEM micrograph, and (b) XRD pattern.

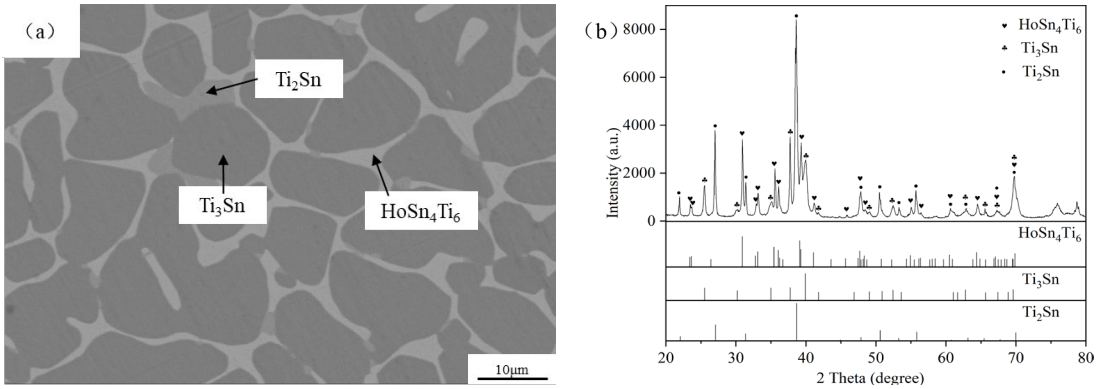

Fig. 8. The experimental results of alloy 3 ($Ho_{2.0}Sn_{3.0}Ti_{68.0}$) heated at 1000 ℃ for 60 days, (a) SEM micrograph, and (b) XRD pattern.

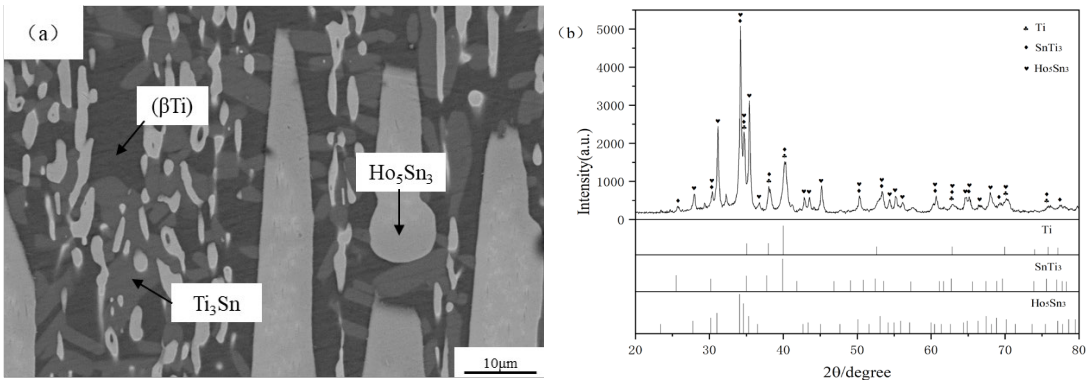

Fig. 9. The experimental results of alloy 2 ($Ho_{17.0}Sn_{18.0}Ti_{65.0}$) heated at 1000 ℃ for 60 days, (a) SEM micrograph, and (b) XRD pattern.

Fig. 10(a) is the SEM micrograph of alloy 1 ($Ho_{28.0}Sn_{5.0}Ti_{67.0}$), and Fig. 10(b) shows its XRD pattern. The coexistence of black (βTi), gray Ho_5Sn_3 and white (Ho) is observed as shown in Fig. 10(a). The gray streak phase is the oxide of Ho_5Sn_3. This indicates that the alloy is located in the three-phase region of (βTi) + Ho_5Sn_3 + (Ho). The XRD of the alloy also confirms the presence of these three phases as shown in Fig. 10(b).

ISSN 2616-5880 Vol. 6, Issue 2: 25-32, DOI: 10.25236/AJMC.2025.060203

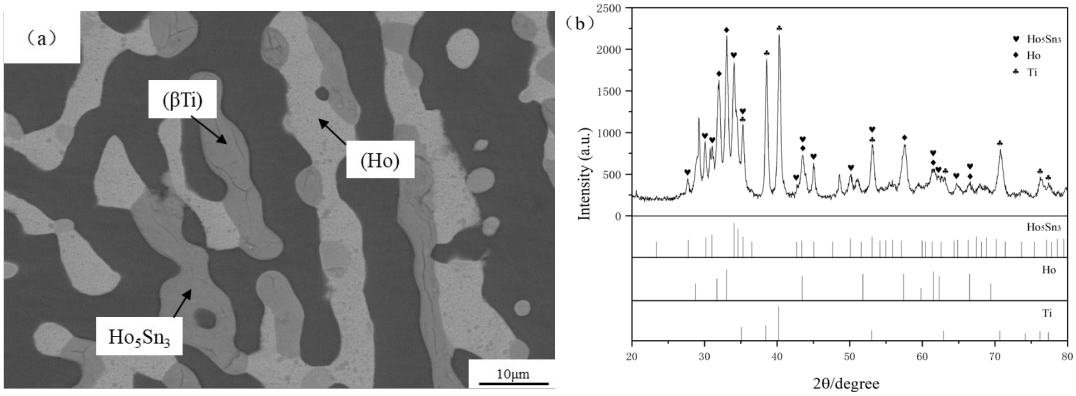

Fig. 10. The experimental results of alloy 1 ($Ho_{28.0}Sn_{5.0}Ti_{67.0}$) heated at 1000 ℃ for 60 days, (a) SEM micrograph, and (b) XRD pattern.

As shown in Table 1, the content of Ti in the Ho_5Sn_3 phase were observed to be 4.2 at.%, 4.3 at.%, and 10.5 at.% for alloys 1-2 and 7, respectively. Here, we have chosen 10.5% as the maximum solubility of titanium in Ho_5Sn_3. No significant solubility was observed in the other binary compounds.

In the Ho–Ti system, it has been confirmed that there is no intermediate compound at 1000 ℃ in this work. In the Ho–Sn system, the existence of the Ho_5Sn_3 was confirmed. This is in agreement with the result of Ref.[7]. The Sn–Ti diagram used for this work was taken from Ref.[12], four binary compounds, namely Ti_6Sn_5, Ti_5Sn_3, Ti_2Sn and Ti_3Sn were observed.

Based on the XRD and SEM/EDS analytical results for all the samples, the phase relationship of the Ho–Sn–Ti ternary system close to the Ho–Ti side at 1000 ℃ was established, as illustrated in Fig. 11.

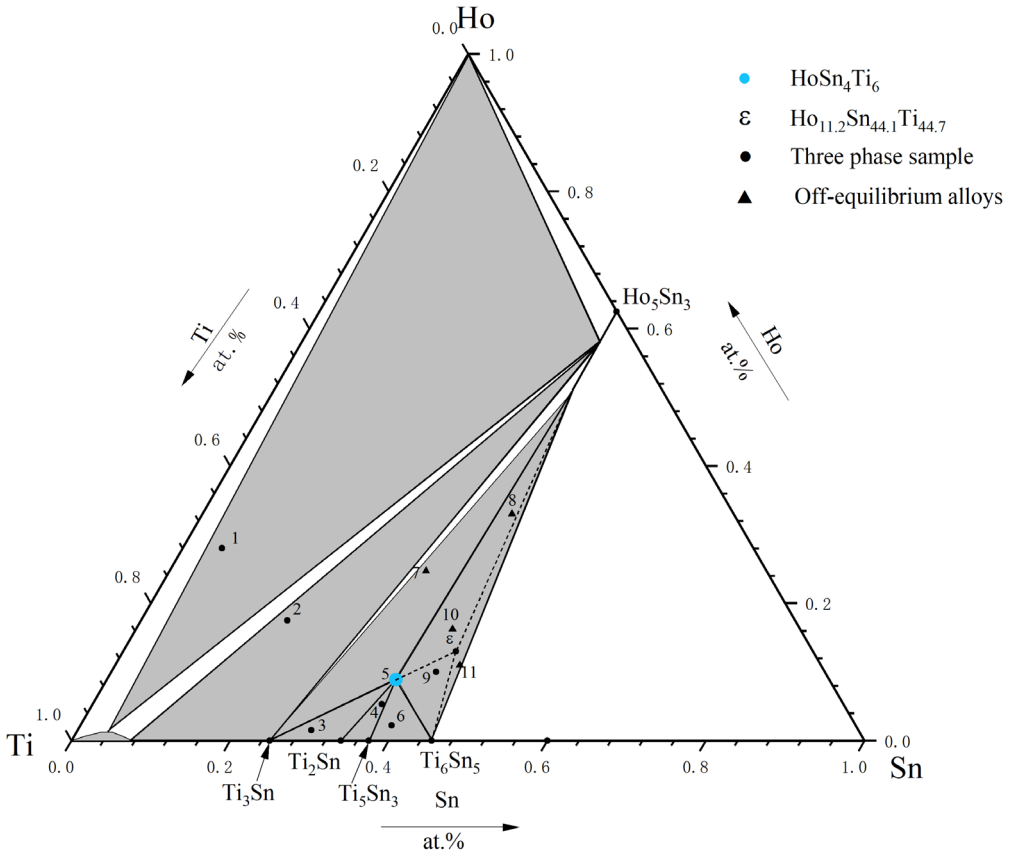

Fig. 11. Isothermal section of Ho–Ti side in the Ho–Sn–Ti system at 1000 ℃.

4. Conclusions

The phase relationship of the Ho–Sn–Ti ternary system close to the Ho–Ti side at 1000 °C was

ISSN 2616-5880 Vol. 6, Issue 2: 25-32, DOI: 10.25236/AJMC.2025.060203

determined. Two new ternary compounds, $HoSn_4Ti_6$ and ε, were discovered. The $HoSn_4Ti_6$ phase belongs to the *R*-3m space group. Its cell parameters were determined to be $a = 0.58178(3)$ nm, and $c = 2.28814(6)$ nm. The ε phase with approximate composition of $Ho_{11}Sn_{44}Ti_{45}$ and unknown structure. The existences of 5 binary compounds (i.e. Ti_6Sn_5, Ti_5Sn_3, Ti_2Sn, Ti_3Sn, Ho_5Sn_3) have been confirmed. The solid solubility of Ti in Ho_5Sn_3 was determined to be about 10.5 at.%. The solid solubility of Ho in the Sn–Ti binary compound is limited.

Acknowledgements

This work was supported by Guangxi Provincial Science and Technology Program (Grant No. 2022KY0150)

References

[1] Peters M, Kumpfert J, Ward C H, et al. Titanium alloys for aerospace applications[J]. Advanced engineering materials, 2003, 5(6): 419-427.
[2] Gooch W A, Ground A P. The design and application of titanium alloys to US Army Platforms-2010[J]. 2010.
[3] Rack H J, Qazi J I. Titanium alloys for biomedical applications[J]. Materials Science and Engineering: C, 2006, 26(8): 1269-1277.
[4] Tekhnol M N. Structure, Phase Composition and Hydrogen Absorption Properties of Multiphase Alloys of Ti–Zr–Mn–V System Alloyed with Holmium[J]. Metallofiz. Noveishie Tekhnol, 2022, 44(7): 913-926.
[5] Hsu H C, Wu S C, Hong Y S, et al. Mechanical properties and deformation behavior of as-cast Ti–Sn alloys[J]. Journal of alloys and compounds, 2009, 479(1-2): 390-394.
[6] Tsao L C, Hsieh M J, Yu Y C. Effects of Sn additions on microstructure and corrosion resistance of heat-treated Ti–Cu–Sn titanium alloys[J]. Corrosion Engineering, Science and Technology, 2018, 53(4): 252-258.
[7] Bulanova M V, Eremenko V N, Petjukh V M, et al. The Ho-Sn (holmium-tin) system[J]. Journal of phase equilibria, 1998, 19: 136-141.
[8] Palenzona A, Manfrinetti P. The tin-rich side of the rare earth-tin systems (R= Gd, Tb, Dy, Ho, Er, Tm, Lu and Y)[J]. Journal of alloys and compounds, 1993, 201(1-2): 43-47.
[9] Sidorko V R, Goncharuk L V. Formation thermodynamics of erbium germanides[J]. Powder Metallurgy and Metal Ceramics, 2008, 47: 702-706.
[10] Romaka L, Romaniv I, Romaka V, et al. Ізотермічний переріз потрійної системи Ho–Cu–Sn при 670 K[J]. Фізика і хімія твердого тіла, 2018, 19(2): 139-146.
[11] Romaka L, Stadnyk Y, Romaka V, et al. Phase equilibria in Ho-Fe-Sn ternary system at 670 K[J]. Physics and Chemistry of Solid State, 2020, 21(2): 272-278.
[12] Murray J L. Phase diagram of titanium alloys[J]. ASM, 1987, 182.
[13] Kuper C, Peng W, Pisch A, et al. Phase formation and reaction kinetics in the system Ti–Sn[J]. International Journal of Materials Research, 2021, 89(12): 855-862.
[14] O'Brien J W, Dunlap R A, Dahn J R. A Mössbauer effect and X-ray diffraction investigation of Ti–Sn intermetallic compounds: II. Nanostructured phases prepared by ball milling with Al2O3 and TiN[J]. Journal of alloys and compounds, 2003, 353(1-2): 65-73.
[15] R-C. Juan, Fullprof suite. Physica B. 192 (1993) 55-69.
[16] Ma J, Zhan Y, She J, et al. The phase relationships in the Gd–Ti–Sn ternary system at 473 K and the new compound $GdSn4Ti_6$[J]. Journal of alloys and compounds, 2010, 489(2): 384-388.